

This is the accepted manuscript made available via CHORUS. The article has been published as:

Excited configurations of hydrogen in the  
 $\text{BaTiO}_{3-x}\text{H}_x$  perovskite lattice associated with  
hydrogen exchange and transport

T. U. Ito, A. Koda, K. Shimomura, W. Higemoto, T. Matsuzaki, Y. Kobayashi, and H.  
Kageyama

Phys. Rev. B **95**, 020301 — Published 31 January 2017

DOI: [10.1103/PhysRevB.95.020301](https://doi.org/10.1103/PhysRevB.95.020301)

# Excited configurations of hydrogen in the $\text{BaTiO}_{3-x}\text{H}_x$ perovskite lattice associated with hydrogen exchange and transport

T. U. Ito<sup>1</sup>, A. Koda<sup>2</sup>, K. Shimomura<sup>2</sup>, W. Higemoto<sup>1,3</sup>, T. Matsuzaki<sup>4</sup>, Y. Kobayashi<sup>5</sup>, and H. Kageyama<sup>5</sup>

<sup>1</sup>*Advanced Science Research Center, Japan Atomic Energy Agency, Tokai, Ibaraki 319-1195, Japan*

<sup>2</sup>*Institute of Materials Structure Science, High Energy Accelerator Research Organization (KEK), Tsukuba, Ibaraki 305-0801, Japan*

<sup>3</sup>*Department of Physics, Tokyo Institute of Technology, Meguro, Tokyo 152-8551, Japan*

<sup>4</sup>*Advanced Meson Science Laboratory, RIKEN, Wako 351-0198, Japan and*

<sup>5</sup>*Department of Energy and Hydrocarbon Chemistry, Graduate School of Engineering, Kyoto University, Nishikyo-ku, Kyoto 615-8510, Japan*

(Dated: December 16, 2016)

Excited configurations of hydrogen in the oxyhydride  $\text{BaTiO}_{3-x}\text{H}_x$  ( $x = 0.1 - 0.5$ ), which are considered to be involved in its hydrogen transport and exchange processes, were investigated by positive muon spin relaxation ( $\mu^+\text{SR}$ ) spectroscopy using muonium ( $\text{Mu}$ ) as a pseudoisotope of hydrogen. Muons implanted into the  $\text{BaTiO}_{3-x}\text{H}_x$  perovskite lattice were mainly found in two qualitatively different metastable states. One was assigned to a highly mobile interstitial protonic state, which is commonly observed in perovskite oxides. The other was found to form an entangled two spin- $\frac{1}{2}$  system with the nuclear spin of an  $\text{H}^-$  ion at the anion site. The structure of the  $(\text{H}, \text{Mu})$  complex agrees well with that of a neutralized center containing two  $\text{H}^-$  ions at a doubly charged oxygen vacancy, which was predicted to form in the  $\text{SrTiO}_{3-\delta}$  perovskite lattice by a computational study [Y. Iwazaki *et al.*, APL Materials **2**, 012103 (2014)]. Above 100 K, interstitial  $\text{Mu}^+$  diffusion and retrapping to a deep defect were observed, which could be a rate-limiting step of macroscopic  $\text{Mu}/\text{H}$  transport in the  $\text{BaTiO}_{3-x}\text{H}_x$  lattice.

PACS numbers: 61.72.-y, 66.30.jp, 76.75.+i

Oxyhydrides of perovskite titanates  $\text{ATiO}_{3-x}\text{H}_x$  ( $\text{A}$ : Ba, Sr, Ca) have attracted much attention because of their fascinating properties, which are associated with the lability of  $\text{H}^-$  ions<sup>1-3</sup>. The perovskite oxyhydrides are obtained as  $\text{O}^{2-}/\text{H}^-$  solid solutions from  $\text{ATiO}_3$  by  $\text{CaH}_2$  reduction. A combined analysis of X-ray and neutron diffraction data on  $\text{BaTiO}_{3-x}\text{H}_x$  ( $x < 0.6$ ) indicates that  $\text{O}^{2-}$  is randomly substituted by  $\text{H}^-$  without creating any detectable amount of vacancies in the anion sublattice. This is in sharp contrast with the established hydrogen configuration in the  $\text{ATiO}_3$  lattice, namely, interstitial protonic hydrogen  $\text{H}_i^+$  bound to an  $\text{O}^{2-}$  ion. The  $\text{O}^{2-}/\text{H}^-$  substitution in  $\text{BaTiO}_3$  suppresses its structural transitions and ferroelectricity; a cubic symmetry is maintained at least down to 2 K. Macroscopic gas analysis revealed that the hydrogen in  $\text{ATiO}_{3-x}\text{H}_x$  is mobile and exchangeable in its gaseous environment at a relatively moderate temperature of  $\sim 400^\circ\text{C}$ . Furthermore,  $\text{CaH}_2$  reduction changes the parent band insulators into paramagnetic metals as evidenced by electrical resistivity and magnetic susceptibility measurements. The transport and hydrogen exchange characters of these materials make them potentially suitable for application in mixed electron/hydrogen ion conductors and hydrogen membranes.

Several theoretical works have been published to date on the stability of hydrogen ions in oxygen-deficient perovskite titanates  $\text{ATiO}_{3-\delta}$  and their transport and exchange mechanisms<sup>4-7</sup>. These studies commonly concluded that the most stable single hydrogen configuration in an n-type carrier-rich environment is  $\text{H}^-$  at a doubly

charged oxygen vacancy  $\text{V}_\text{O}^{2+}$ , formally expressed as  $\text{H}_\text{O}^+$ . On hydrogen kinetics starting from the  $\text{H}_\text{O}^+$  configuration, two types of scenarios were proposed. One is based on the idea of correlated migration of  $\text{H}_\text{O}^+$ ,  $\text{V}_\text{O}^{2+}$ , and  $\text{O}_\text{O}^0$  in the network of the anion site<sup>1</sup>. The other involves charge-state transitions between  $\text{H}_\text{O}^+$  (hydridic) and  $\text{H}_i^+$  (protonic). Releasing two electrons to the conduction band, the hydride in the  $\text{H}_\text{O}^+$  center can be transformed to the highly mobile  $\text{H}_i^+$ , and it then diffuses as a proton from one interstitial site to another separated by a low potential barrier<sup>4,6</sup>. After that, it finds another  $\text{V}_\text{O}^{2+}$  center and converts back to  $\text{H}_\text{O}^+$  with two electrons. This scenario explains the hydrogen transport and exchange abilities of  $\text{ATiO}_{3-x}\text{H}_x$  well, without involving migration of the other heavy elements. Some calculations dealt with an interaction between an  $\text{H}_\text{O}^+$  center and an incoming  $\text{H}_i^+$ , which should be taken into account when considering hydrogen transport and exchange in highly hydrogenated  $\text{ATiO}_{3-x}\text{H}_x$ <sup>5,6</sup>. Three metastable configurations were theoretically proposed for two hydrogen atoms at the  $\text{V}_\text{O}^{2+}$  center. The simplest one is an  $\text{H}_2$  molecule-like state, labeled as  $(\text{H}_2)_\text{O}^{2+}$ . The others are antisymmetric  $(2\text{H})_\text{O}^0$  and symmetric  $(2\text{H})_\text{O}^0$  states involving two hydrogen ions in the hydride form, proposed by Iwazaki *et al.* in  $\text{SrTiO}_{3-\delta}$ <sup>5</sup>. These centers could be converted to and back from an  $(\text{H}_i^+ + \text{H}_\text{O}^+)$  defect combination with relatively low activation energy. Because the  $\text{H}_i^+$  center is highly mobile, one can consider another path for hydrogen transport and exchange in  $\text{ATiO}_{3-x}\text{H}_x$  via the metastable  $(\text{H}_2)_\text{O}^{2+}$ ,  $(2\text{H})_\text{O}^0$ , or  $(2\text{H})_\text{O}^0$  states.

In contrast to theoretical advancements, experimental

insights into the mechanisms of hydrogen transport and exchange in  $\text{ATiO}_{3-x}\text{H}_x$  are still quite limited. In this paper, we report on an experimental investigation of excited hydrogen configurations in the  $\text{BaTiO}_{3-x}\text{H}_x$  lattice by the positive muon spin relaxation ( $\mu^+\text{SR}$ ) method, which would be associated with the hydrogen kinetics in it. The  $\mu^+\text{SR}$  technique has been widely utilized for the study of local electronic structures of hydrogen impurities in condensed matter. Spin-polarized positive muons implanted into a solid lose their kinetic energy mainly by ionization and are then trapped at local potential minima, not necessarily at the global minimum. The electronic structure of muonium (a hydrogen-like  $\mu^+e^-$  bound state: Mu) is supposed to be very similar to that of hydrogen except for a small correction due to the difference in reduced mass ( $\sim 0.4\%$ ). The as-implanted mixture of Mu states is far from equilibrium and can involve metastable excited states<sup>8</sup>. In the  $\text{BaTiO}_{3-x}\text{H}_x$  lattice, most implanted muons are expected to mimic excited configurations of hydrogen together with  $\text{H}^-$  in the host lattice through their lifetime. This is because the cross section to produce a Mu analog of the most stable  $\text{H}_\text{O}^+$  center should be quite small owing to the low concentration of vacancies in the anion sublattice. Information on local electronic structures and atomic configurations around the muons can be obtained from the time evolution of muon spin polarization, which is driven by magnetic interactions between a muon spin and surrounding nuclear and electron spins.

Powder samples of  $\text{BaTiO}_{3-x}\text{H}_x$  ( $x=0.1, 0.2, 0.3$ , and  $0.5\pm0.05$ ) with an average grain diameter of  $0.17\ \mu\text{m}$  were prepared from  $\text{BaTiO}_3$  powders by a  $\text{CaH}_2$  reduction method<sup>1</sup>.  $\mu^+\text{SR}$  experiments were carried out using the DQ1 spectrometer in the D1 area, J-PARC MUSE, Japan, and the Argus spectrometer in the Port 2, RIKEN-RAL, UK. The  $\text{BaTiO}_{3-x}\text{H}_x$  powder was compressed into a pellet and glued with Apiezon N grease on a silver sample holder that was mounted on a conventional  $^4\text{He}$ -flow cryostat. Pulsed  $\mu^+\text{SR}$  measurements were performed in a zero applied field (ZF) and longitudinal magnetic fields (LF) over the temperature range 15–450 K. A double-pulsed surface muon beam was incident to the sample. The time interval between two muon bunches in each spill was 600 ns for J-PARC MUSE and 324 ns for RIKEN-RAL. The time evolution of muon spin polarization  $P(t)$  was extracted from the forward-backward asymmetry of positrons emitted during the decay of positive muons. The origin of the time  $t$  was set to the arrival time of the second bunch and data after  $t = 0$  were analyzed. The influence of the double-pulsed time structure on  $P(t)$  was taken into account according to the treatment given in Ref.<sup>9</sup>.

We first discuss the  $x$  dependence of ZF- $\mu^+\text{SR}$  spectra for  $\text{BaTiO}_{3-x}\text{H}_x$ . Figure 1 shows a ZF- $\mu^+\text{SR}$  spectrum of as-prepared  $\text{BaTiO}_{3-x}\text{H}_x$  samples at 15 K, together with an LF- $\mu^+\text{SR}$  spectrum of the  $x = 0.5$  sample at 50 Oe. The constant background from muons that missed the sample was identified by using a reference sample and

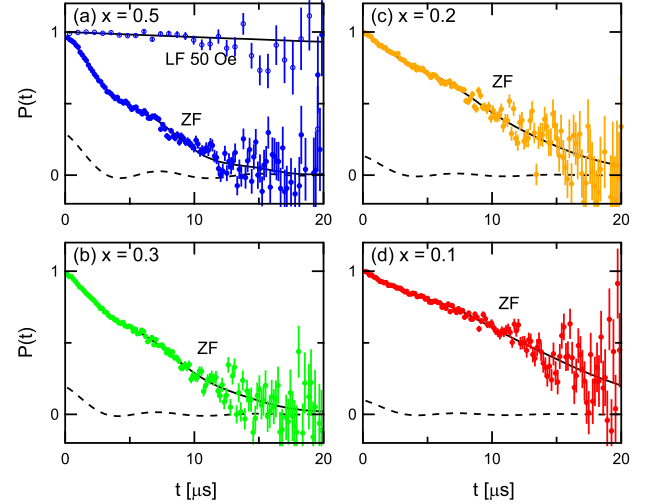


FIG. 1. ZF- $\mu^+\text{SR}$  spectra of (a)  $x = 0.5$ , (b)  $x = 0.3$ , (c)  $x = 0.2$ , and (d)  $x = 0.1$  samples at 15 K. The solid curves show the best fits to Eq. (3). Partial contribution from the 2S component is displayed by the broken curves. A LF- $\mu^+\text{SR}$  spectrum of the  $x = 0.5$  sample in a LF of 50 Oe was also shown in Fig. 1(a) together with an exponential fitting curve.

has been subtracted from the spectra. There was no sign of paramagnetic  $\text{Mu}^0$  in the ZF- $\mu^+\text{SR}$  spectra of  $\text{BaTiO}_{3-x}\text{H}_x$  in contrast to the parent band insulator  $\text{BaTiO}_3$ , where shallow-donor  $\text{Mu}^0$  was detected below  $\sim 80\ \text{K}$ <sup>10</sup>. The absence of  $\text{Mu}^0$  in  $\text{BaTiO}_{3-x}\text{H}_x$  is consistent with its metallic conductivity, since conduction electrons screen the positive charge of  $\mu^+$  and prevent an electron from localizing around it.

Muon spin relaxation in ZF is mainly caused by quasi-static magnetic interactions between a diamagnetic muon ( $\text{Mu}^+$  or  $\text{Mu}^-$ ) and surrounding nuclei, since the polarization is mostly recovered by applying a small LF of 50 Oe, as shown in Fig. 1(a). The muon spin depolarization curves in ZF have an oscillating feature superposed on a Gaussian relaxation curve. Such spontaneous oscillation is usually regarded as evidence of coherent magnetic order. However, this is clearly not the case, since there is no sign of magnetic order in the temperature dependence of magnetic susceptibility down to 2 K<sup>1</sup>. Strong coupling between a muon spin and a small number of nearby nuclear spins also causes such an oscillation in ZF- $\mu^+\text{SR}$  spectra even in nonmagnetic or paramagnetic materials<sup>11–17</sup>. In  $\text{BaTiO}_{3-x}\text{H}_x$ , the oscillating component is ascribed to the coupling between a muon spin ( $S = \frac{1}{2}$ ) and a nearby  $^1\text{H}$  nuclear spin ( $I = \frac{1}{2}$ ), since  $^1\text{H}$  has a large nuclear dipole moment in comparison with those of stable Ba and Ti nuclei<sup>18</sup>. Considering the low concentration of  $^1\text{H}$ , we ignore the situation where more than two  $^1\text{H}$  nuclear spins equally couple to a muon spin as a collinear  $^{19}\text{F}-\mu^+-^{19}\text{F}$  spin configuration<sup>11,12</sup>. The muon spin relaxation function for the entangled two spin-

$\frac{1}{2}$  state (hereafter, referred to as 2S) is expressed as

$$G_{2S}(t) = \frac{1}{6} + \frac{1}{6} \cos(2\pi f_d t) + \frac{1}{3} \cos(\pi f_d t) + \frac{1}{3} \cos(3\pi f_d t), \quad (1)$$

$$f_d = \frac{\mu_0 \hbar \gamma_\mu \gamma_I}{2d^3}, \quad (2)$$

where  $d$  is the distance between  $\mu^+$  and  $^1\text{H}$  at the anion site and  $\gamma_\mu$  and  $\gamma_I$  are the gyromagnetic ratios of  $\mu^+$  and  $^1\text{H}$  ( $\gamma_\mu/2\pi = 135.53$  MHz/T and  $\gamma_I/2\pi = 42.58$  MHz/T), respectively<sup>12,13</sup>. On the other hand, the Gaussian relaxation component is ascribed to diamagnetic muons that do not create such a special magnetic bond with a single  $^1\text{H}$ . These muons should be located further from  $\text{H}_\text{O}^+$  centers than those in the 2S state and lose their spin polarization via magnetic dipolar interactions with a large number of surrounding nuclei. In such a case, the Gaussian Kubo-Toyabe relaxation function (relaxation rate  $\Delta$ ) based on local field approximation is useful<sup>19</sup> and its early-time region ( $t < 2\Delta^{-1}$ ) is well approximated by the Gaussian function  $e^{-\Delta^2 t^2}$ .

The ZF- $\mu^+$ SR spectra at 15 K were fitted to the following function, including the 2S and Gaussian components, i.e.,

$$P(t) = p_{2S} e^{-\lambda t} G_{2S}(t) + (1 - p_{2S}) e^{-\Delta^2 t^2}, \quad (3)$$

where  $\lambda$  and  $p_{2S}$  are the relaxation rate and the fraction of the 2S state, respectively. The exponential function phenomenologically describes spin relaxation of the 2S state<sup>16</sup>, which can be caused by inhomogeneity, surrounding nuclei, and slow dynamics. Satisfactory fits were obtained, as shown in Fig. 1 with solid curves. Figure 2 shows the  $x$  dependences of  $f_d$ ,  $p_{2S}$ ,  $\lambda$ , and  $\Delta$ , obtained from the fits. The distance of 2S spins,  $d$ , is also shown in Fig. 2(a), calculated from  $f_d$  via Eq. (2). The linear increase in  $p_{2S}$  suggests that the formation probability of the 2S state is proportional to the hydrogen concentration. The constant  $d$  is reasonable because the local structure of the 2S state should be independent of  $x$  for such low hydrogen concentrations. The average length,  $1.64(1)\text{\AA}$ , is much shorter than the distance between two nearest-neighbor (nn) anion sites,  $\sim 2.8\text{\AA}$  and much longer than the bond length of a hydrogen molecule,  $0.74\text{\AA}$ . This indicates that the 2S state can be assigned neither to a  $(\text{Mu}_\text{O}^+, \text{H}_\text{O}^+)$  defect combination over two nn anion sites, nor a molecular  $\text{MuH}$  center at a doubly charged oxygen vacancy. On the other hand, the average value of  $d$  agrees well with the theoretical H-H distances for the  $(2\text{H})_\text{O}^0$  and  $(2\text{H})_\text{O}^0$  centers in  $\text{SrTiO}_{3-\delta}$ ,  $1.67$  and  $1.64\text{\AA}$ , respectively<sup>5</sup>. Because the Ba and Sr compounds have almost the same lattice constant, it seems reasonable to ascribe the 2S state to one of the  $\text{Mu}^-$  analogs of these centers, namely,  $(\text{Mu}, \text{H})_\text{O}^0$  or  $(\text{Mu}, \text{H})_\text{O}^0$ , as shown in Fig. 2(e). Our observation demonstrates that the uncommon  $(2\text{H})_\text{O}^0$  or  $(2\text{H})_\text{O}^0$  center, where the hydrogen exchange can occur, is really

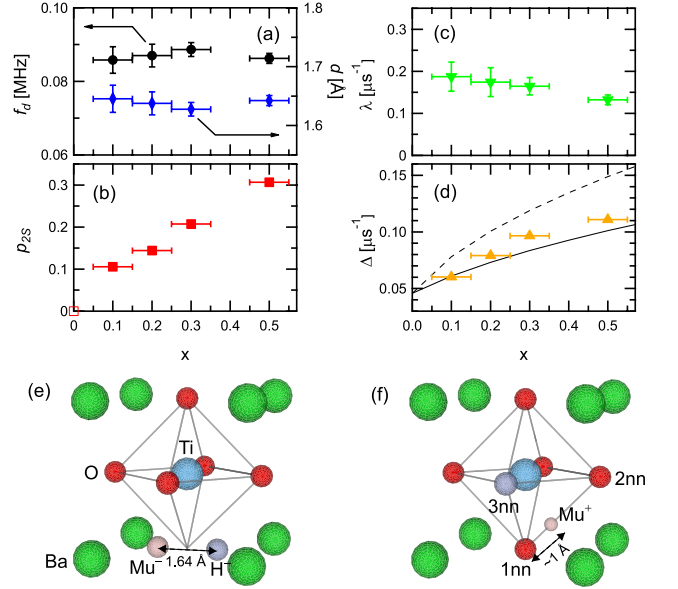


FIG. 2.  $x$  dependences of (a)  $f_d$  and  $d$ , (b)  $p_{2S}$ , (c)  $\lambda$ , and (d)  $\Delta$  at 15 K in ZF, and the most probable atomic configurations associated with (e) the 2S component and (f) the Gaussian component.

allowed to form in the n-type perovskite lattice at least as a metastable state. This center is also important in carrier-control technology for transition-metal oxides because the  $\text{V}_\text{O}^{2+}$  donor can be completely passivated by forming this with hydrogen<sup>5</sup>.

The  $\Delta$  included in the Gaussian component monotonically increases with increasing  $^1\text{H}$  concentration, as shown in Fig. 2(d). This behavior can be quantitatively explained by assigning the Gaussian component to a  $\text{Mu}^+$  analog of the  $\text{H}_i^+$  center bound to an  $\text{O}^{2-}$  ion. Here we assume a simplified atomic configuration as illustrated in Fig. 2(f);  $\text{Mu}_i^+$  is placed on an edge of the anion octahedron in the undistorted perovskite lattice with a lattice constant of  $4.02\text{\AA}$  and the O-Mu bond length is set to  $0.987\text{\AA}$ , based on a first-principles calculation on the structure of the  $\text{H}_i^+$  center in cubic  $\text{BaTiO}_3$ <sup>4</sup>. The first nn anion is fixed to be  $\text{O}^{2-}$  to form the O-Mu bond and  $\text{O}^{2-}$  at the third nn and further anion sites is randomly replaced by  $\text{H}^-$  with a probability of  $x/3$ . Under these conditions, we calculated the rms width  $\sigma (= \Delta/\gamma_\mu)$  of the local field distribution at the  $\text{Mu}_i^+$  site for the following two cases with regard to the second nn anion configuration: (i) always  $\text{O}^{2-}$ , (ii) randomly replaced by  $\text{H}^-$  with a probability of  $x/3$ . The  $\Delta(x)$  curves for cases (i) and (ii) were obtained from the relation:  $\Delta = \gamma_\mu \sigma$ , as shown in Fig. 2(d) with solid and broken lines, respectively. While both curves reproduce the increasing trend of the experimental data, the agreement is even better for case (i). This suggests that a nearly collinear O-Mu...H configuration ( $\text{H}^-$  at the 2nd nn anion site) is unstable and, even if it forms, it immediately falls into the  $(\text{Mu}, \text{H})_\text{O}^0$  or  $(\text{Mu}, \text{H})_\text{O}^0$  state, as shown in Fig. 2(e).

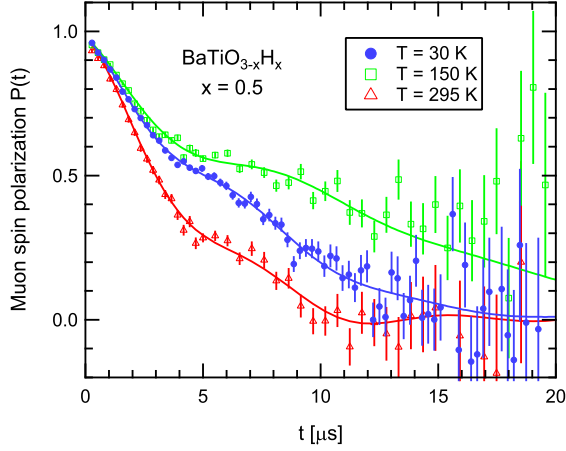


FIG. 3. ZF- $\mu^+$ SR spectra of  $\text{BaTiO}_{2.5}\text{H}_{0.5}$  ( $x = 0.5$ ) at 30, 150, and 295 K. The solid curves show the best fits to Eq. (3).

We then move on to the temperature dependence of ZF- $\mu^+$ SR spectra in  $\text{BaTiO}_{2.5}\text{H}_{0.5}$  ( $x = 0.5$ ). Figure 3 shows ZF- $\mu^+$ SR spectra of the as-prepared sample at 30, 150, and 295 K. The spectrum rises with increasing temperature from 30 to 150 K and then falls as a result of further warming to 295 K. In spite of the peculiar temperature dependence, the two-component feature (2S and Gaussian) seems to be retained within the temperature range of our experiment. We therefore used Eq. (3) to fit the ZF spectra and obtained satisfactory fits, as shown in Fig. 3 with solid curves. The parameters  $f_d$ ,  $d$ ,  $p_{2S}$ ,  $\lambda$ , and  $\Delta$  obtained by the fits are shown in Fig. 4 as functions of temperature. Closed and open symbols show data taken before and after keeping the sample at 450 K for four hours in a cryostat vacuum, respectively. No significant influence of the four-hour annealing is observed in Fig. 4, indicating that the  $\text{H}_\text{O}^+$  configuration in the host lattice was maintained during the experiment and thus the temperature variation of the spectra should be primarily attributed to muon kinetics.

Moderate temperature dependences in  $d$  and  $p_{2S}$  for the 2S component indicates that conversion between the 2S and the  $\text{Mu}_i^+$  states seldom occurs below 450 K. This suggests that higher temperature is necessary to activate the hydrogen exchange process proposed by Zhang *et al.*<sup>6</sup> On the other hand, the  $\Delta$  for the Gaussian component shows a notable temperature dependence with double plateaus separated by a concave at around 150 K. Similar behavior was reported in Sc-doped  $\text{SrZrO}_3$ , explained within the framework of a two-state model on interstitial  $\text{Mu}^+$  diffusion<sup>20,21</sup>. Here, we adopted a simplified version of this model, as was used in Ref.<sup>22</sup>. In this framework, muons are assumed to start in the  $\text{Mu}_i^+$  site with a static Gaussian width  $\Delta_0$  and diffuse between equivalent sites with activation energy  $E_a$  and attempt rate  $\nu_0$ . They are then captured with a probability  $c$  per hop at a deep trap site with a static Gaussian width  $\Delta_1$  and stay there until they decay. We numerically eval-

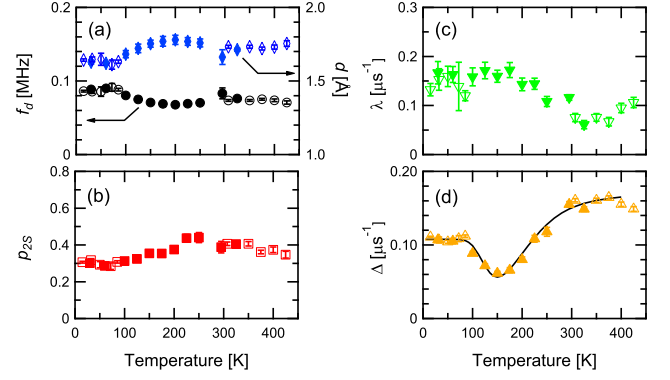


FIG. 4. Temperature dependences of (a)  $f_d$  and  $d$ , (b)  $p_{2S}$ , (c)  $\lambda$ , and (d)  $\Delta$  in ZF for  $\text{BaTiO}_{2.5}\text{H}_{0.5}$ . The solid curve in (d) is the best fit to the simplified two-state model (see text).

uated  $\Delta(T)$  as a function of  $\Delta_0$ ,  $\Delta_1$ ,  $E_a$ ,  $\nu_0$ , and  $c$ , and fitted it to the experimental  $\Delta$  in the temperature range 15–400 K with  $\Delta_0$  fixed at  $0.108 \mu\text{s}^{-1}$  (the average value of  $\Delta$  below 85 K). Consequently, we obtained the best fit curve, as shown in Fig. 4(d), and the following parameters:  $\Delta_1 = 0.175(3) \mu\text{s}^{-1}$ ,  $E_a = 0.086(4) \text{ eV}$ ,  $\nu_0 = 10(3) \times 10^8 \text{ s}^{-1}$ , and  $c = 0.025(4)$ . The value of  $E_a$  is close to that in Sc-doped  $\text{SrZrO}_3$ <sup>20</sup>, demonstrating the validity of our analysis. This is about half the calculated potential barrier height of  $\sim 0.2 \text{ eV}$  for interstitial diffusion of protons in cubic  $\text{BaTiO}_3$ <sup>6</sup>. The difference could be the consequence of a higher vibrational zero-point energy for the muon<sup>20,23</sup>. The increase in  $\Delta$  above 150 K corresponds to the trapping of the highly mobile  $\text{Mu}_i^+$  at the deep trap site with a static Gaussian width  $\Delta_1$ , which is considerably larger than  $\Delta_0$ . This might be a rate-limiting step of macroscopic  $\text{Mu}/\text{H}$  conduction in  $\text{BaTiO}_{3-x}\text{H}_x$ . The large  $\Delta_1$  suggests a high density of hydrogen around the deep trap and thus a  $\text{Mu}$  capture at  $\text{V}_\text{O}^{2+}$  is unlikely.

It should be noted that our methodology cannot deal with the case of direct  $\text{H}^-$  migration in the network of anionic octahedra<sup>1</sup>. Our experimental results never exclude such a process, which is considered to be more or less activated at high temperature and contribute to net  $\text{H}$  transport together with other possible processes.

In conclusion, we investigated excited hydrogen configurations allowed in the  $\text{BaTiO}_{3-x}\text{H}_x$  lattice by the  $\mu^+$ SR spectroscopy. Our experimental results are mostly in line with a theoretical proposal on hydrogen exchange and transport involving charge-state transitions<sup>4–6</sup>, but also indicate the existence of a deep  $\text{Mu}/\text{H}$  trap and its importance in macroscopic  $\text{Mu}/\text{H}$  transport. It remains for future studies to fully identify this deep trap.

## ACKNOWLEDGMENTS

We thank T. Sakaguchi and D. Tomono for technical assistance and Y. Iwazaki and K. Nishiyama for helpful discussions. This work was supported by CREST, JST and the MEXT KAKENHI Grant No. 24108509 and the JSPS KAKENHI Grant No.24710101.

- 
- <sup>1</sup> Y. Kobayashi, O. J. Hernandez, T. Sakaguchi, T. Yajima, T. Roisnel, Y. Tsujimoto, M. Morita, Y. Noda, Y. Mogami, A. Kitada, M. Ohkura, S. Hosokawa, Z. Li, K. Hayashi, Y. Kusano, J. Kim, N. Tsuji, A. Fujiwara, Y. Matsushita, K. Yoshimura, K. Takegoshi, M. Inoue, M. Takano, and H. Kageyama: *Nature Mater.* **11**, 507-511 (2012).
  - <sup>2</sup> T. Yajima, A. Kitada, Y. Kobayashi, T. Sakaguchi, G. Bouilly, S. Kasahara, T. Terashima, M. Takano, and H. Kageyama: *J. Am. Chem. Soc.* **134**, 8782-8785 (2012).
  - <sup>3</sup> N. Masuda, Y. Kobayashi, O. Hernandez, T. Bataille, S. Paofai, H. Suzuki, C. Ritter, N. Ichijo, Y. Noda, K. Takegoshi, C. Tassel, T. Yamamoto, and H. Kageyama: *J. Am. Chem. Soc.* **137**, 15315-15321 (2015).
  - <sup>4</sup> Y. Iwazaki, T. Suzuki, and S. Tsuneyuki, *J. Appl. Phys.* **108**, 083705 (2010).
  - <sup>5</sup> Y. Iwazaki, Y. Gohda, and S. Tsuneyuki, *APL Materials* **2**, 012103 (2014).
  - <sup>6</sup> J. Zhang, G. Gou, and B. Pan: *J. Phys. Chem. C* **118**, 17254-17259 (2014).
  - <sup>7</sup> J.B. Varley, A. Janotti, and C.G. Van de Walle: *Phys. Rev. B* **89**, 075202 (2014).
  - <sup>8</sup> R. L. Lichti, K. H. Chow, and S. F. J. Cox: *Phys. Rev. Lett.* **101**, 136403 (2008).
  - <sup>9</sup> T. U. Ito, W. Higemoto, K. Ohishi, K. Satoh, Y. Aoki, S. Toda, D. Kikuchi, H. Sato, and C. Baines: *Phys. Rev. B* **82** 014420 (2010).
  - <sup>10</sup> T. U. Ito, W. Higemoto, T. D. Matsuda, A. Koda, K. Shimomura: *Appl. Phys. Lett.* **103**, 042905 (2013).
  - <sup>11</sup> J. H. Brewer, S. R. Kreitzman, D. R. Noakes, E. J. Ansaldo, D. R. Harshman, and R. Keitel: *Phys. Rev. B* **33**, 7813 (1986).
  - <sup>12</sup> K. Nishiyama, S. W. Nishiyama, and W. Higemoto: *Physica B* **326**, 41-45 (2003).
  - <sup>13</sup> T. Lancaster, S. J. Blundell, P. J. Baker, M. L. Brooks, W. Hayes, F. L. Pratt, J. L. Manson, M. M. Conner, and J. A. Schlueter: *Phys. Rev. Lett.* **99**, 267601 (2007).
  - <sup>14</sup> J. S. Lord, S. P. Cottrell, W. G. Williams: *Physica B* **289-290**, 495-498 (2000).
  - <sup>15</sup> R. Kadono, K. Shimomura, K. H. Satoh, S. Takeshita, A. Koda, K. Nishiyama, E. Akiba, R. M. Ayabe, M. Kuba, and C. M. Jensen: *Phys. Rev. Lett.* **100**, 026401 (2008).
  - <sup>16</sup> J. Sugiyama, Y. Ikeda, T. Noritake, O. Ofer, T. Goko, M. Månsson, K. Miwa, E. J. Ansaldo, J. H. Brewer, K. H. Chow, and S. Towata: *Phys. Rev. B* **81**, 092103 (2010).
  - <sup>17</sup> T. U. Ito, W. Higemoto, K. Ohishi, N. Nishida, R. H. Heffner, Y. Aoki, A. Amato, T. Onimaru, and H. S. Suzuki: *Phys. Rev. Lett.* **102**, 096403 (2009).
  - <sup>18</sup> N. J. Stone: *At. Data Nucl. Data Tables* **90**, 75-176 (2005).
  - <sup>19</sup> R. S. Hayano, Y. J. Uemura, J. Imazato, N. Nishida, T. Yamazaki, and R. Kubo: *Phys. Rev. B* **20** 850 (1979).
  - <sup>20</sup> R. Hempelmann, M. Soetratmo, O. Hartmann, and R. Wäppling: *Solid State Ionics* **107**, 269-280 (1998).
  - <sup>21</sup> M. Borghini, T. O. Niinikoski, J. C. Soulié, O. Hartmann, E. Karlsson, L. O. Norlin, K. Pernestål, K. W. Kehr, D. Richter, and E. Walker: *Phys. Rev. Lett.* **40**, 1723-1726 (1978).
  - <sup>22</sup> J. S. Lord and W. G. Williams: *Solid State Ionics* **145**, 381-385 (2001).
  - <sup>23</sup> T. Norby: *Solid State Ionics* **40-41**, 857-862 (1990).